Quantum annealing: near future applications

Final Degree Project for Physics Enginnering

By Oscar Escolano Rubio

Tutor: Prof. Jordi Boronat Medico

from Univeritat Politecnica de Catalunya

Director: Prof. K. Birgitta Whaley

from University of California Berkeley

Contents

1 Introduction **1**

2 Main concepts **2**

2.1 Qubit and the Bloch Sphere 2

2.2 Von Neumann equation and Lindblad master equation 4

2.3 Weak, continuous measurement 7

2.4 Quantum backaction 9

2.5 Quantum Zeno effect 9

2.6 Computing science concepts 10

2.6.1 Complexity of a problem 10

2.6.2 Optimization problems 11

2.7 Quantum annealing 12

2.8 Quantum Approximate Optimization Algorithm(QAOA) 14

2.9 Adiabatic & diabatic 16

2.10 Stoquastic Hamiltonians 16

3 Current State-of-the-art and discussion **17**

3.1 Stoquastic vs non-Stoquastic Hamiltonians 18

3.2 QAOA vs Quantum Annealing 19

3.3 Adiabatic Quantum computing 20

3.4 General quantum annealing approaches 21

4 Simulation of a qubit **22**

4.1 Introduction 22

4.2 Calculations 23

4.3 The Pierre Rouchon Method 25

4.4 Results 26

4.5 Side remark 30

5 Conclusion **31**

6 Acknowledgements **32**

A Autocorrelation and the Telegraph signal **33**

B References **36**

1 Introduction

Quantum annealing is one of the most relevant topics among the quantum computing scholars at the moment. The recent developments in neighboring fields such as quantum memories[1] and error correction[2] seem to give hope to achieving the desired "quantum supremacy", the era when quantum will surpass classical computing. In the last decades, there has been an exponential growth in computing power, known as the Moore's law[3], mainly due to the miniaturization techniques developed and refined these years. But this is bound to reach its physical limitations in the next years[4]. All of this means that quantum computing will probably have a strong position in computationally expensive applications.

To surpass the classical computing doesn't only imply faster calculations, it would even mean to get results to problems that classically would take astronomically large times to solve, such as NP-hard problems, considered unsolvable in a practical sense. Even though some projects have brought us nearer to quantum supremacy (such as Google's Quantum computer[5] or IBM Quantum Experience[6]), there's still plenty of room to improve. One of the areas of the vast field of quantum computing that seems most promising in the near future is quantum annealing. The quantum approach gives us new tools that are currently being developed by researchers all around the globe to tackle more complex problems and try to outperform the classical algorithms. These algorithms have to deal with huge search spaces and datasets, rendering the problem computationally intensive in the solution search. So, quantum parallelisation is a big intrinsic advantage that is used to explore the entire solution space in a global approach, leading to avoiding local minima. This is important because the solution space usually is non-convex, meaning that there might be several suboptimal solutions, which are not desired (except in some specific cases such as approximation algorithms). Also, in many problems the search space is discrete, where gradient descent fails to find the optimal solution, so quantum optimization is an explored option.

In this project, we will be explaining the main concepts of quantum computing, discussing the state-of-the-art and making a qubit simulation with Rabi drive under continuous measurement. So, the goal is to make a complete introduction to the foundations of this broad research field.

2 Main concepts

In this section we will review the main concepts involving quantum annealing and its essential components to understand the topic. We won't be explaining all the quantum mechanics concepts, since it's background knowledge from Physics Engineering. However, more specific concepts will be explained. We will start explaining some advanced quantum mechanics concepts, followed by some Computer Science concepts of interest to our project. We will end explaining some Quantum Computing terminology to get an in-depth picture.

2.1 Qubit and the Bloch Sphere

A qubit is the basic unit of information, analogous to the classical bit, in the quantum frame. This is represented by a two-state system. While a bit can only be either 0 or 1, a qubit is a linear superposition of both states.

$$|\Psi\rangle = \alpha\,|0\rangle + \beta\,|1\rangle \tag{1}$$

Since this is a quantum state, it follows the same interpretation as described in quantum mechanics: α and β are the probability amplitude for each state respectively and they follow the normalization rule ($|\alpha|^2 + |\beta|^2 = 1$). The pair $|0\rangle$, $|1\rangle$ form a basis for a single qubit, usually called the computational basis. In the physical world, this usually corresponds to the ground ($|0\rangle$) and excited ($|1\rangle$) states of an electron, a photon or an ion (sometimes it's used the polarization or the spin). For a better visualization and understanding of a qubit, it is common practice to use the Bloch Sphere representation (fig. 2). The Bloch sphere uses the normalisation of α and β to its advantage, because, by using a change of coordinates and ignoring the global phase of a qubit, one can represent every pure state in the surface of a sphere. These new coordinates of the Bloch sphere are given by:

$$\alpha = cos(\theta/2) \tag{2}$$

$$\beta = e^{i\phi} sin(\theta/2) \tag{3}$$

Notice that the angle inside the sine and cosine are divided by 2. So, orthogonal quantum states

will be antipodal in this representation. For instance, the state $|0\rangle$ is at the top of the sphere and the state $|1\rangle$ is at the bottom.

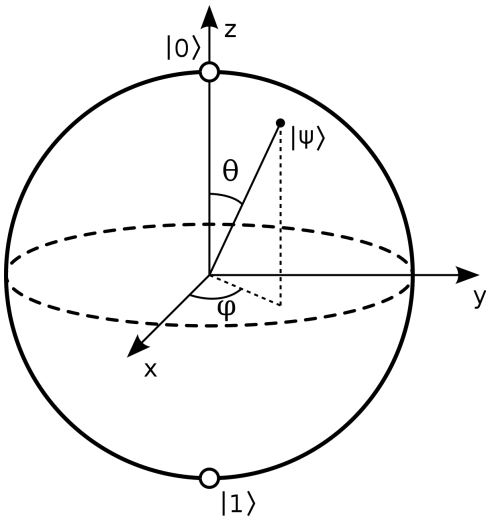

Figure 2: Bloch Sphere representation

All pure states will remain in the surface of the Bloch Sphere. However, if there are perturbations to the system from the environment and cause decoherence, the qubit might be in a mixed state. Mixed states are represented inside the Bloch Sphere, so now we have to take into account a third coordinate: the radius (r). The mixed state or the statistical mixture of incoherent states is represented by equation [4], where p_i is the probability of being in the state $|\Psi_i\rangle$.

$$\rho = \sum_i p_i \left|\Psi_i\right\rangle \left\langle\Psi_i\right| = \begin{pmatrix} \rho_{00} & \rho_{01} \\ \rho_{10} & \rho_{11} \end{pmatrix} \tag{4}$$

It also has the constraints of $Tr(\rho) = 1$, it is a positive matrix (so the eigenvalues are all positive $\rho > 0$) and it has to be a Hermitian matrix. In the equation [4], we have stated the more general version of a mixed state and the particular case of a single qubit system.

In order to manipulate qubits, one must use quantum logic gates. These operators are unitary, and therefore, are reversible. They correspond to rotations to the Bloch sphere. The most notable

examples are the Pauli matrices.

$$\begin{aligned} \sigma_x &= X = \begin{pmatrix} 0 & 1 \\ 1 & 0 \end{pmatrix} \\ \sigma_y &= Y = \begin{pmatrix} 0 & -i \\ i & 0 \end{pmatrix} \\ \sigma_z &= Z = \begin{pmatrix} 1 & 0 \\ 0 & -1 \end{pmatrix} \end{aligned} \tag{5}$$

They are rotations of π radians of the Bloch sphere in each respective axis. If we take the computational basis as stated before, each rotation has a distinct role. The X-gate is called *bit-flip*, since it swaps the amplitude probabilities of each state. In the classical limit, if one had a 0 it would be changed to a 1 after the transformation, corresponding to a NOT gate. The Z-gate is also called *phase-flip*, since it shifts the phase of β by π radians. The Y-gate, apart from being the π radians rotation in the y-axis, can be obtained by applying a X-gate, a Z-gate and a global phase to the qubit.

$$Y = iXZ \tag{6}$$

The global phase of the qubit is not relevant in single-qubit systems but it becomes relevant in multi-qubit systems, since there will be relative phases between different qubits.

2.2 Von Neumann equation and Lindblad master equation

The time evolution of a closed quantum state is given by the Schrödinger equation.

$$i\hbar\partial_t |\Psi\rangle = H |\Psi\rangle \tag{7}$$

Where H is the Hamiltonian of the system.

However, many times we have a more complex system and cannot use only pure states. We usually have to work with mixed states, since there's decoherence involved in practical scenarios. So, in order to work with these statistical mixtures we use the density operator and its associated time

evolution equation: the von Neumann equation. One can derive this equation by differentiating the density operator and applying the Schrödinger equation to each bra and ket. The von Neumann equation is:

$$\partial_t \rho = -i/\hbar[H, \rho] \tag{8}$$

Sometimes it is expressed in reduced units $\hbar = 1$. One could say that the von Neumann equation is a more generalized version of the Schrödinger equation. But even if it's more general and allows us to work with mixed states, it is derived for closed systems, so it doesn't take into account all the factors that may be involved in our system, such as the noise from the environment or the possible quantum backaction it might have from a detector. For these purposes, one has to use a more general master equation: the *Linblad master equation*.

$$\partial_t \rho = -i/\hbar[H, \rho] + \sum_{n,m=1}^{N^2-1} h_{nm} \left(A_n \rho A_m^\dagger - \frac{1}{2} \left\{ A_m^\dagger A_n, \rho \right\} \right) \tag{9}$$

Where the $\{A_n\}$ is an orthonormal basis in the Hilbert space and $A_{N^2} = \mathbb{1}$, h_{nm} is a component of the positive semidefinite matrix h and the symbol $\{A, B\} = AB + BA$ is the anticommutator.

The frame to derive it is as follows. We have our system of interest in a Hilbert space ($\mathcal{H}$) and its environment ($\mathcal{H}_E$). So, we can use the von Neumann equation to the total system, that includes both the environment and the qubit, and derive the evolution of the subsystem of the qubit. So, the Hamiltonian is divided into three parts: the environment (H_E), the qubit (H_S) and the interaction between them (H_I).

$$H_T = H_S \otimes \mathbb{1}_E + \mathbb{1}_S \otimes H_E + \lambda H_I \tag{10}$$

Here, λ is the strength of interaction. When the Lindblad equation is derived, we make several important assumptions. One is that the strength of this interaction is small ($\lambda << 1$). Another assumption is that at some point in time, there is no correlation between the environment and the system. Thus, there's some instant (that is taken as $t = 0$) where $\rho_T(0) = \rho_S(0) \otimes \rho_E(0)$, so the density matrix is separable. A third assumption is that the environment at this starting point is a

thermal bath, so it follows is a Boltzmann ensemble.

$$\rho_E(0) = \frac{e^{-H_E/k_BT}}{\mathrm{Tr}\left[e^{-H_E/k_BT}\right]} \tag{11}$$

In fact, since the interaction is weak, we also suppose that the environment state will always remain thermal. This is a big assumption that implies two things. The first one is that the timescale of the correlation(τ_C) and relaxation(τ_I) of the environment are much smaller than the timescale of the system(τ_S), so that in the frame of the system we see spontaneous changes. The second thing implied is that the system and the environment are always decoupled ($\rho_T(t) = \rho_S(t) \otimes \rho_E(0)$). This is a strong assumption, since we know that there is an interaction Hamiltonian, so they surely cannot be fully decoupled. But, since the system and environment work in different timescale regimes, from a physical point of view it makes sense to take into account only the scale of interest. In fact, this supposition is what allows us to focus only in the system subspace in the derivation of the Lindblad master equation.

Finally, the last assumption made is the rotating wave approximation, where the high frequency terms are neglected and we only keep the resonant terms. This means that the eigenvalues that act at the interaction timescale, and therefore are much faster than the system timescale ($\tau_I << \tau_S$) will be neglected and we only keep the terms that match the system timescale.

Even though the derivation of the Lindblad equation is not the subject of our project, it is important to understand all the concepts surrounding its formalism and derivation. So, we will take a brief time to talk about the *interaction picture*. The interaction (or Dirac) picture is a unitary transformation applied to the states and operators of a system, similar to the Heisenberg and Schrödinger pictures. While the Schrödinger picture places all the time dependency on the state vectors and the Heisenberg picture does it on the observables, the interaction picture remains in the middle ground. It gives part of the time dependency to observables and another part to the state vector. It is really convenient to use when the Hamiltonian consists in two or more parts (such as Eq. [10]): one that we can solve if it were a close system (H_S) and one that it is more difficult and generally constitutes part of an open system(H_E and H_I). The state and the operators will evolve with the system Hamiltonian,

which makes it easier to perform calculations on it:

$$|\psi_{\mathrm{I}}(t)\rangle = \mathrm{e}^{iH_S t/\hbar}\,|\psi_{\mathrm{S}}(t)\rangle \tag{12}$$

$$A_{\mathrm{I}}(t) = e^{iH_S t/\hbar} A_{\mathrm{S}}(t) e^{-iH_S t/\hbar} \tag{13}$$

Where the sub-indexing of the states(ψ) and observables(A) are the Schrödinger(S) and interaction(I) pictures. Notice that we use the same Hamiltonian as in the Schrödinger picture.
So, this picture is really useful for performing derivations in open systems, since we just use the part of the Hamiltonian that we know how to work with. It is commonly used as a transition to be able to perform some integrations of the full system in an easier way and then get back to the Schrödinger picture of the system we are interested in.

2.3 Weak, continuous measurement

In the Quantum Physics course we saw that to measure a quantum state we had to project it using an observable. The state would then collapse into one of the eigenstates with the probability associated to it, as stated in the third postulate. This type of measurements are called *von Neumann measurements*. This means that we lose all the other information contained in the quantum system but obtain a certain result. For many applications, such as in quantum computing, we want to obtain information from the system but at the same time try to keep the system perturbation to the minimum. This can be accomplished by methods called *weak measurements*. Weak measurements are measurements that use the interactions of the system with an external device to get partial information and don't cause the collapse of all the system we are interested in. An important remark to make before continuing the explanation is that it doesn't violate any quantum postulate (as expected), so it can be fully explained by quantum theory.
So, in order to perform the weak measurement, our system has to have a unitary interaction with an external system. Then, we perform a von Neumann measurement on the external system to obtain a result from it. This measurement is formalized as generalized measurements called *positive operator valued measure (POVM)*. With this information and knowing the interaction between both systems

we can get partial information on the state of our system. If the uncertainty is big, it's called a *weak measurement*. On the other hand, if the uncertainty is small, it's called a *strong measurement*.

Having this new approach to measurement, we can perform an almost continuous measurement by dividing the time in small timesteps ($\Delta t \to 0$) and performing weak measurements in each of them. Therefore, we obtain an information of the state of our system in an almost continuous way. However, in this process of taking the limit to 0 we have to approximate the measurement into a stochastic parameter, in Eq. 14 it's α_s (see [7] for a mathematical derivation).

$$\alpha_{\mathrm{s}} = \langle X \rangle + \frac{\Delta W}{(8k)^{1/2}\Delta t} \tag{14}$$

Where $\langle X \rangle$ is the mean of the non-stochastic variable, W is a zero-mean random Gaussian variable with variance Δt and k is a measurement strength parameter (the higher the value of k, the stronger the measurement is).

This is the price to pay for continuous information, a non-deterministic result. Now, the evolution of the system will be governed by a stochastic master equation (SME) and it will define the quantum trajectory ($\rho(t)$).

Even more uncertainty arises when the detector is used in a real scenario where it does an *inefficient measurement*. An inefficient measurement occurs when the detector isn't able to pick all the signal measurement or when this signal is comparable to the thermal noise and it's not distinguishable. When this happens, the way to tackle this problem is as if there was two measurements at the same time but one is unknown. This way, we take into account that there are some timesteps that the system evolves due to the interaction of a detector but we don't know the result of it. This procedure leads to the rise of a new parameter: *detector efficiency* (η), that is the ratio of known signal to total signal of the measurement performed.

Taking into account all these conditions, one can derive a general master equation for continuous measurements (assuming they form Gaussian noise as consequence of the detector-system interaction), as done in [7](p.12). This is the most general version with uncorrelated Wiener noise.

$$\mathrm{d}\rho = -\frac{\mathrm{i}}{\hbar}[H,\rho]\mathrm{d}t + \sum_n \left(\mathcal{D}\left[c_n\right]\rho \mathrm{d}t, + \eta_n^{1/2}\mathcal{H}\left[c_n\right]\rho \mathrm{d}W \right) \tag{15}$$

We see that the first part is the same as in the von Neumann deterministic equation. Afterwards, we get the summed terms over the n observers: $\mathcal{D}$ are the disturbance terms caused by the *backaction* and the $\mathcal{H}$ are the information terms that we gained by each detector. The differential dW are uncorrelated Wiener processes. Notice that even if we gain information or not, the detector makes a disturbance just for being there.

2.4 Quantum backaction

The quantum backaction is the disturbance generated by a detector making a measurement on the system. It must be taken into account in any weak measurement device, since it will change the dynamics of our qubit. It is the first step to introducing the dynamics of open quantum systems, that commonly cause decoherence in some way.

One of the consequences of quantum backaction is the degradation of purity of the system. As we are using the Lindblad master equation, the purity fulfills that $\frac{d}{dt}\left(\mathrm{Tr}\left[\rho^2\right]\right) \leq 0$. This means that any pure state will become more and more mixed as time passes.

2.5 Quantum Zeno effect

Another interesting concept that appears in quantum computing research is the quantum Zeno effect. When we make a measurement, we project the state into an eigenstate of the observable. Therefore, if one is able to make fast enough measurements, the state of the system will remain in the eigenstate and the system won't be able to evolve in time. This is an interesting phenomena that has been explored as a tool to control qubit trajectories [8]. They made a setup that allowed to perform measurements along different axis of the Bloch sphere. Then, by doing continuous enough measurements one can drag the state in the eigenstate. However, this approach has its limitations. The time-energy uncertainty principle (the alternative form of the uncertainty principle) imposes an intrinsic restriction to this problem.

$$\Delta E \cdot \Delta t \geq \frac{\hbar}{2} \tag{16}$$

One could think of making measurements with a difference in time of Δt and make it as small as possible to accomplish a continuous measurement. But this principle inherent in quantum mechanics shows that it would lead to making the energy fluctuate to the point where it could jump from the ground state to the excited state, thus rendering the qubit uncontrollable. So, overall, there are some limitations to this approach if one was trying to take this to the limit.

In [8], Hacohen-Gourgy *et al.* explore the capabilities of quantum Zeno effect in dragging a state as they desire while suppressing the motion due to Hamiltonian evolution. Using a continuous measurement (as we have explained in section 2.3), they are able to keep the qubit in an eigenstate and know if it has escaped the desired trajectory, as a form of error detection. Therefore, they use the measurement not only to drag the state, but also to maintain the information of its position updated. Their results indicate that there was a dragging rotation speed that was optimal for high fidelity results, meaning that going faster lead to more stray trajectories and going slower didn't improve the performance. They also remarked that if the goal is to reach a certain state faster with high fidelity, one could also be more restrictive on the post-selection threshold (i.e. be more strict with the threshold for the stochastic signal, since we diminish the effect of randomness).

2.6 Computing science concepts

In order to get a better picture of the quantum computing research, we will briefly define some of the most important computing science concepts that we have encountered.

2.6.1 Complexity of a problem

The complexity in computer science refers to the amount of computational resources that are needed to solve a problem. There are multiple ways to analyze the complexity of a problem. In the early quantum computing, knowing how many logical gates and qubits were needed to run an algorithm was of the uttermost importance to set good foundations in the field, since it was a well studied area in classic computing and we could easily compare with. The classical computing allows for non-reversible operations, while quantum computing must be performed with reversible transformations

until the measurement is done. This meant that the classical gates AND, OR, NAND, *etc.* had to be reinvented or adapted to fulfill this constraint, since they were not reversible.

But, as stated in [9], one can construct any classical circuit that had t gates and s bits into a reversible circuit with $O(t^{1+\epsilon})$ gates and $O(s)$ bits. This way of counting how many gates and bits are needed to implement an algorithm is what is called *quantum circuit complexity*. It is the most common way to refer to the complexity of a problem in quantum computing but not the only one. When talking about algorithm one can also talk about its *quantum query complexity*. The quantum query complexity is the number of calls that are needed to perform to an oracle to perform a calculation. An oracle is a black-box in a circuit, that given an input it gives an output with a certain transformation but we don't know or discuss how it's done inside of it. Therefore, the query complexity is usually useful for establishing lower bounds to a problem, since the oracle will probably increase the complexity. Finally, another type of complexity is given by the *communication complexity*, that only takes into account the number of qubits needed to perform a calculation.

More generally, one can classify algorithms by its complexity class. The complexity class denotes the asymptotic behaviour of an algorithm when an input parameter tends to infinity ($N \to \infty$). For instance, some of the complexity classes are P, NP, NP-hard. The P class stands for polynomial, meaning it can solve the problem in polynomial time. The class NP stands for non-deterministic polynomial, and it means that for the instances that solve the problem one can verify it in polynomial time. If $P \neq NP$, then NP-hard problems cannot be solved in polynomial time. As its name indicates, they are the more complex class and, therefore, need the most resources to be soved. Many optimization problems fall into this category.

2.6.2 Optimization problems

An optimization problem deals with finding the best solution to a problem. By best solution it is meant to be the minimum or maximum of a certain function (depending if it is a *minimization* or *maximization* problem, respectively). This is a broad field that comprises many different problems. When the problem is a minimization problem, this function is usually referred to it as *error function* or *objective function*; and when the problem is a maximization problem is usually referred as

evaluation score function. Formally, these functions $f(x)$ can be as complex as one desires as long as they map $f : R^n \to R$ and the possible results make sense within some boundaries (constraints)[10]. But, usually, the more complex problems have to be simplified in order to be feasible and practical. Also, notice that there are several optimization problems that deal with discrete functions, such as the travelling salesman problem (TSP), the minimum spanning tree (MST) or many other combinatorial optimization problems. This is relevant because we will see that quantum approximated optimization algorithm works in discrete environments.

A combinatorial optimization problem (COP) tries to find an optimal object from a finite set of objects [11]. Usually, the problem scales with exponential or superpolynomial laws, so they are outside the P complexity class (usually within NP class). Therefore, finding the solution using brute force by checking all the possible solutions one by one is not a smart approach. This is where the parallelism in quantum methods gives a hint it could be beneficial to solve these problems. For instance, the TSP is a problem where you have to choose the optimal path to go to around all the cities without repetition. So, from all the possible paths we have to choose the shortest one. This problem scales as $O(N!)$ in a naive approach, so it would be impossible to calculate efficiently in a completely random way. The most efficient classical algorithm to find an exact solution is of order $O(n^2 2^n)$[12], so, it is common to use algorithms using heuristics and approximations[13].

2.7 Quantum annealing

Quantum annealing refers to a series of procedures and methods that try to find the solution of a problem using quantum fluctuations. This is a global procedure, that avoids the local minima of the function and in the limit of infinite time the system reaches the global minimum of the function. This differs from classical local approaches very popular to solve many problems in recent days, such as gradient descent. Quantum annealing's idea rises from its classical counterpart: simulated thermal annealing. Thermal annealing is a method that tries to overcome the problems local convergence methods give. When it usually would get stuck in a local minima, we induce a stochastic fluctuation (as if it were a thermal fluctuation, hence the name) in order to jump a potential barrier and be able to search new minimum. In the case of quantum annealing, these fluctuations are quantum fluctuations

that imitate quantum tunneling. So, it is expected that for steep potential barriers, quantum annealing outperforms its classical counterpart. Quantum annealing is usually implemented using adiabatic quantum computing (AQC), that is based on the adiabatic theorem[14]. The adiabatic theorem was formulated by M. Born and V. Fock in 1928 and it stated:

> *"A physical system remains in its instantaneous eigenstate if a given perturbation is acting on it slowly enough and if there is a gap between the eigenvalue and the rest of the Hamiltonian's spectrum."*

In practice, this means that if one lets evolve a system with a sufficiently slow pace, it will remain in the ground state throughout the whole process. This is really useful in Quantum annealing, in fact, it's the principle that allows this techniques. The system is initially prepared in the ground state of a Hamiltonian H_0. It is usually a simple Hamiltonian that makes it easy to prepare its ground state. If it's possible, it is useful to use a superposition of all states as a primer(the initial guess), so the solution will naturally explore the whole space of solutions. The system is then evolved through a time-dependent Hamiltonian until it reaches the final Hamiltonian H_1. The ground state of H_1 needs to have encoded the information of the desired solution. So, the whole Hamiltonian is usually represented as follows:

$$H(s) = (1 - A(s))\, H_0 + A(s) H_1 \tag{17}$$

Where s is a re-scaled time that goes from 0 (corresponding to the initiation of the annealing t_0) to 1 (corresponding to the ending of the annealing t_f) and A(s) is a monotonically increasing function that satisfies $A(0) = 0$ and $A(1) = 1$. It is not the only structure proposed to perform Adiabatic Quantum Computing but a simple case to start with[15]. There are many difficult parts in this process. One of them is finding the right Hamiltonian H_1 that will have the solution encoded in it. Many problems can be reformulated in other terms as long as they are mathematically equivalent. This is done in many combinatorial problems as we will see in later sections of this project. Another problem one can encounter is that during this transition from the H_0 Hamiltonian to the H_1 Hamiltonian the energy gap between the ground state and the first excited state becomes too small. When this happens, we have to slow down the computation to remain in the ground state. This will also be discussed in later sections with some recent research.

2.8 Quantum Approximate Optimization Algorithm(QAOA)

QAOA is a computational method that combines classical and quantum designs to tackle difficult problems such as combinatorial optimization problems[16]. It was first proposed in 2014, by Edward Farhi and Jeffrey Goldstone with promising results. From there, many other algorithms combining quantum and classical computation have been proposed. These methods usually try to get a result close to the optimal result, but they don't ensure the optimal result in a better time than other algorithms. In order to understand how it works, lets analyze the original QAOA. As a maximization problem, it can be written as:

$$z_f = \arg\max_z C(z) \quad \text{where} \quad C(z) = \sum_{\alpha=1}^{m} C_\alpha(z) \tag{18}$$

Each C_α is a logical clause. A logical clause is a combination of bits (that can be negated with a NOT gate) that are united with AND gates. For instance, a clause would be: $C_1 = b_1 \cap b_6 \cap \bar{b}_9$, and it would mean that this clause would be TRUE(1) only if the bits 1 and 6 are equal to 1 and the bit 9 is equal to 0. Any other combination would output a 0 for this clause. The $C(z)$ function that we want to maximize is the sum of all causes. Then, we define the unitary cost function operator $U(C, \gamma)$ as:

$$U(C, \gamma) = e^{-i\gamma C} = \prod_{\alpha=1}^{m} e^{-i\gamma C_\alpha} \tag{19}$$

We also define another unitary operator $U(B, \beta)$ as:

$$U(B, \beta) = \prod_{j=1}^{n} e^{-i\beta\sigma_j^x} \tag{20}$$

This operator is the product of commuting single bit σ_x operations. Notice that the eigenstate of this operator is the $|s\rangle = \prod_{i=1}^{n} |+\rangle_i$, so it's a mixing-state Hamiltonian.

We start the algorithm by applying p times these two operators (one can apply different rotations by changing γ and β at each step):

$$|\gamma, \beta\rangle = U(B, \beta_p)U(C, \gamma_p)...U(B, \beta_1)U(C, \gamma_1) |s\rangle \tag{21}$$

In an intuitive sense, this last step is applying the cost function and then remixing the system many times in small steps. Then we calculate the mean value of $C(z)$ in the current state.

$$F_p(\boldsymbol{\gamma}, \boldsymbol{\beta}) = \langle \gamma, \beta | \, C \, | \gamma, \beta \rangle \tag{22}$$

Finally we can define the magnitude M_p as the maximum of M_p over the angles. One can prove (as done in [16]) the following:

$$\lim_{p \to \infty} M_p = \max_z C(z) \tag{23}$$

Therefore, if one evaluates that magnitude several times (in fact is of order $O(m \log m)$ to get a good enough result with high probability) and obtains the maximum, it will approximate asymptotically the solution that we are looking for.

To obtain the optimal constant angles $(\boldsymbol{\gamma}, \boldsymbol{\beta})$ one has to solve a simple optimization problem (by solving a linear system) classically before doing any quantum calculation.

This algorithm was proven to beat the classical algorithms at that time (2014). Unfortunately for QAOA, a few months later, in 2015, a new classical algorithm was released that outperformed QAOA's results [17]. However, the QAOA set an important precedent that inspired many other methods.

QAOA is really useful for MaxCut problems. A MaxCut problem is stated as trying to find a cut that partitions a graph in two subsets of vertices with the maximum number of edges cut. An interesting and useful fact about MaxCut problems is that it is equivalent to minimizing the Hamiltonian of an Ising Model of spin glass:

$$H(s) = - \sum_{i,jNN} J_{ij} s_i s_j \tag{24}$$

So, this was an indicator that maybe this method (QAOA) or some variant could be implemented in similar complex physical systems and other areas. In fact it has been useful for other problems, such as a new method for calculating the eigenvalues using a quantum approach [18] or in a method called Quantum Alternating Operator Ansatz that is a generalisation of QAOA's operators [19].

One of the variants of QAOA was implemented in quantum neural networks(QNN) [20]. However,

in a 2018 article [21], it was demonstrated that classical-quantum hybrid large systems that started with a random circuit, without a better prior, could get easily stuck in *barren plateaus*. A barren plateau is a part of solution space where the gradient is exponentially small and at the same time is a wide potential barrier so it doesn't update in any direction and gets trapped. So, one of the main issues is finding a good prior considering the architecture of the QNN to avoid these areas.

2.9 Adiabatic & diabatic

Adiabatic quantum annealing, as explained before, is the process of finding the minimum of a function using a process where the quantum state remains always on the ground state to achieve the result. It is the most largely explored branch of the field, since the adiabatic theorem ensures a good theoretical asymptotic convergence and there's an efficient classical simulation of quantum annealing associated with it. On the other hand, diabatic quantum annealing permits to make the optimization using excited states that have a non-zero energy gap between them. It is not as widely researched as the adiabatic counterpart but, as we will see in a state-of-the-art comparison, it seems to be the most promising for future research.

2.10 Stoquastic Hamiltonians

A term one can find in the literature of quantum simulations is the *stoquasticity* of a Hamiltonian. It should not be confused with *stochasticity* (that refers to a randomly induced Hamiltonian). A stoquastic Hamiltonian is characterized by having their off-diagonal matrix elements in the standard computational basis as real and non-positive values. This is really important in the fields of condensed matter and quantum chemistry, where one needs to simulate fermions and the "sign-problem" arises. The sign-problem occurs when one tries to map from quantum to classical a system of fermions, because it produces a partition function with some positive, negative and complex Boltzmann weights, that have no physical meaning. Therefore, one cannot perform a Monte Carlo simulation on this system (unless one can find a suitable change of basis that avoids this problem). A stoquastic Hamiltonian avoids the sign problem, so are more easy to simulate [22].

In a more rigurous way, a k-local stoquastic Hamiltonian is

$$H = \sum_{i=1}^{M} H_i \tag{25}$$

where every H_i matrix is a hermitian operator that acts on, at most, k qubits and satisfies that

$$\langle x| H |y\rangle \leq 0 \quad \forall x, y \in \{0,1\}^n \quad \text{with} \quad x \neq y \tag{26}$$

The notation $\{0,1\}^n$ is used for a n-bits string. Notice that the Boltzmann exponential operator $e^{-\beta H_i}$ (that is used for Monte Carlo simulations) has non-negative matrix elements for any positive inverse temperature (β). Also, $\langle x| e^{-\beta H_i} |y\rangle$ depends only non-trivially on the bits of x and y. Therefore, one can approximate its quantum partition function ($Tre^{-\beta H}$) using a classical partition function with local non-negative Boltzmann weights using the Suzuki-Trotter formula, for instance. So, one can make more easily a classical simulation of a quantum system when it has a stoquastic than a non-stoquastic Hamiltonian.

This means that Quantum Monte Carlo simulations are able to follow the instantaneous ground state of the said Hamiltonian and, therefore, produce the similar results at a similar computational cost as adiabatic quantum computing, differing by a polynomial law.

3 Current State-of-the-art and discussion

In this section we will talk about the current state of the art on several fields surrounding quantum annealing and its applications. We will cover a recent discovery concerning stoquastic and non-stoquastic Hamiltonians, a discussion between quantum approximate optimization algorithms and quantum annealing, the state-of-the-art of adiabatic quantum computation and a comparison between adiabatic and diabatic quantum computation.

3.1 Stoquastic vs non-Stoquastic Hamiltonians

As we saw in one of the previous sections, stoquastic Hamiltonians are easier to implement in a classical setup because they have an almost direct way to be simulated in classical Quantum Monte Carlo methods[23]. And the standard quantum adiabatic optimization has been demonstrated to work in stoquastic Hamiltonians. So, there were speculations that the increased complexity of non-stoquastic Hamiltonians could give a quantum speedup advantage for adiabatic quantum optimization.
In "De-Singing Hamiltonians for Quantum Adiabatic Optimization", E. Crosson *et al.*[24] find a way to compare its possibilities and share its conclusions. They introduce a one-on-one mapping transformation for every non-stoquastic Hamiltonian ($H(s)$ in previous notation) that ends in a classical Hamiltonian (H_1) to a stoquastic adiabatic path. They found that non-stoquastic Hamiltonians had a smaller spectral gap than stoquastic Hamiltonians. This means that on an adiabatic quantum computation, the stoquastic Hamiltonians will take less time than non-stoquastic ones, in a general scenario.

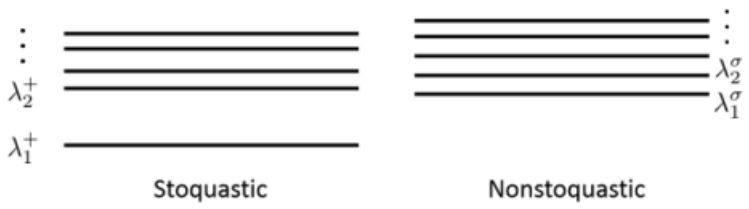

Figure 3: Intuitive comparison between the non-stoquastic and stoquastic eigenvalues shown in [24]

The conclusion of the study was that non-stoquastic Hamiltonians do not have an implicit advantage over stoquastic Hamiltonians. However, carefully crafted non-stochastic paths, have been demonstrated to be more efficient in some cases [25]. So, every case must be carefully studied but, in a general case, it has been refuted that non-stoquastic Hamiltonians will be the key that will inherently give an enormous advantage to adiabatic quantum computing.

3.2 QAOA vs Quantum Annealing

As we have seen, QAOA and Quantum Annealing have some similarities. In fact, in the limit $p \to \infty$ the QAOA is equivalent to Adiabatic Quantum Computing (Eq.23). QAOA is largely explored for low p values, but remains unclear its performance on $p >> 1$. As stated in this article [26], when the minimum spectral gap is very small, QAOA's results are much better than those acquired by Adiabatic Quantum Annealing (in fact several orders of magnitude). This is because it can be optimized to use a diabatic procedure, overcoming the problem of having to stay on the ground state when the gap is so small. In this sense, the QAOA behaves like an optimized path of diabatic Quantum Annealing, discretized via trotterization. Trotterization is the process of breaking the sum of exponentiated non-commuting Hamiltonians into repeated products of the different Hamiltonians applied in small angles.

$$e^{(A+B)} = \lim_{n\to\infty} \left(e^{\frac{A}{n}} e^{\frac{B}{n}}\right)^n \tag{27}$$

QAOA is similar to a finite trotterisation of the Quantum Annealing system. One could think of applying Adiabatic quantum annealing more quickly so the probability of finding the global minimum is diminished but run it several times and then take the minimum of those results. To see what is the optimal balance there is a parameter called *time-to-solution* (TTS).

$$TTS \propto \frac{\log[1 - p_d]}{\log[1 - p_s(t_f)]} \tag{28}$$

It depends on the desired probability of being in the ground state (p_d) and the success probability of a single-instance run of the algorithm at the end of the attempt($p_s(t_f)$). In really small spectral gaps the TTS is independent of the energy gap in both Quantum Annealing and QAOA (Fig.4). This result also suggests that TTS in Quantum Annealing could be improved exponentially if they were implemented diabatically instead of adiabatically. In this sense, the future research could focus on this aspect.

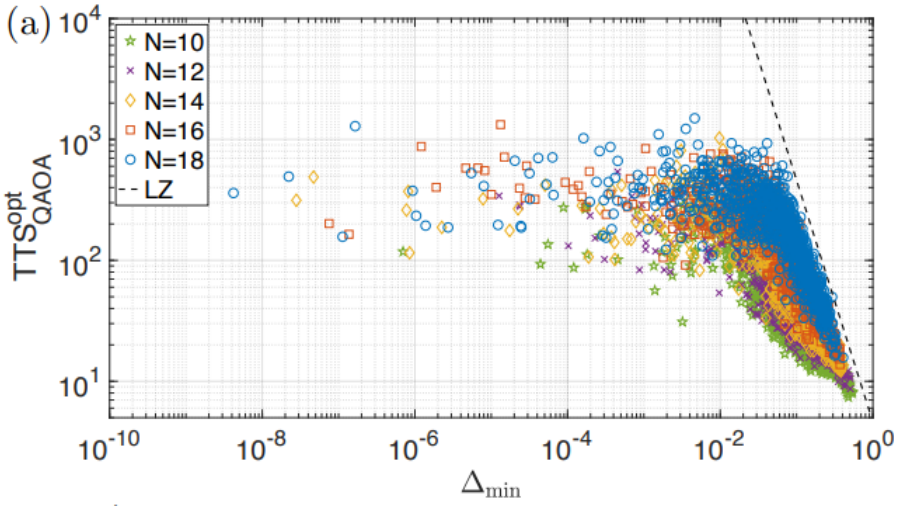

Figure 4: Results from the article [26], where we can see the relation between TTS and the minimum spectral gap. Notice that for small gaps the TTS remains almost constant

3.3 Adiabatic Quantum computing

The key of Adiabatic Quantum Computing is the gap between the excited state and the ground state during all the annealing. As derived in this review on Adiabatic Quantum Computing by A. Lidar and T. Albash[27], the time needed to successfully perform an annealing can be estimated to be proportional to the inverse gap squared ($t_f \propto 1/(\Delta E)^2$). If the gap becomes small, it is easier to jump and leave the ground state, therefore not being Adiabatic Quantum Computing. In this case, if one wants the computation to stay guided by the adiabatic principle, the computation has to be slowed down to let it relax all the times to the ground state. It is in these scenarios where the Adiabatic Quantum Computing doesn't provide a speedup on classical computing.

Another interesting fact is that it has a direct comparison with a classical metaheuristic: *thermal annealing* or *simulated annealing(SA)*. In thermal annealing the jumps are randomly generated by simulating thermal fluctuations. This means that it is easier for the system to make low energy leaps, but if the potential profile is high it will be difficult to surpass it and it is more likely to remain in a local minimum. In Quantum Annealing, the jumps are probabilistic governed by the laws of QM. This means that the solution is able to jump higher potentials, rendering Quantum Annealing more powerful in several instances than SA, as seen in the article by B. Heim *et al.*[28].

Adiabatic quantum computing has been largely explored because it is sustented by the Adiabatic theorem, that ensures asymptotical convergence of the method. Even though it hasn't delivered yet the promise speedup, it has set a good theoretical foundation that enables to continue exploring its capabilities and can be used in neighbooring fields.

3.4 General quantum annealing approaches

We have focused on adiabatic quantum annealing, but there exist other types, such as *diabatic quantum annealing*. Even though it's not the goal of our project to go in-depth in this topic, we will explain a little bit what it consists on and the future possibilities. As explained in [29], the diabatic quantum annealing allows the state to jump to excited states in the Hamiltonian path to obtain the result. The key to this method is to have an energy gap in some of the excited states. This way, we can restrict the "solution path" to a subspace: a band (with a bandgap to higher states). As stated in the theorem given in [30] for a diabatic path, the error is bounded proportionally to the inverse of run-time ($\propto \frac{1}{t_f}$). Also, the more states there are in the band(d) and the bigger that band is (δ), the more error one will have. So, diabatic computation, in order to be practical and be able to perform efficient results it has to fulfill $d = O(1)$ & $\delta = O(1)$. This way, we have a more general definition compared to the adiabatic quantum computing (that only allows $\delta = 0$).

Diabatic quantum annealing opens a new world of possibilities, since there are not known classical simulations associated with it. In the adiabatic case, one can make approximations to the quantum Monte Carlo method (as we have seen in a previous section). So, it suggests that it might allow for algorithms that have an enhanced performance: the quantum speedup. For instance, some steps have been made in [31], where they implemented a MAX-2-SAT problem (a NP-hard problem) with 20 qubits and outperformed the adiabatic procedure with a computation time several orders of magnitude smaller. They noticed the gap between the ground state (which had encoded the solution) and the first state was really small at one point, an avoided crossing. If they had started in the ground state and wanted it to remain in it, they would have had to go slow, in order to avoid a jump. However, they prepared the prior in the first excited state. And when it arrives at the crossing, the population of states change. This change is caused by a phenomena called *Landau-Zener effect*. The

Landau-Zener effect for a two-state system is characterized by the transition probability:

$$P = \exp\left(-2\pi \frac{|\mathrm{H}_{12}|^2}{\hbar(dE/dt)}\right) \tag{29}$$

where H_{12} is the off-diagonal matrix element that controls the transition probability, usually given by thermal fluctuations or other perturbations. We can see that as $dE/dt \to 0$, $P \to 0$. That means that the faster we perform the annealing, the bigger the transition probability of its population. So, an adiabatic transition can only be performed in a slow procedure. So, in their experiment, they arrived with a 5% probability of being in the ground state in a time 3 orders of magnitude smaller than in the adiabatic case. This made the diabatic process far more efficient, because one could repeat the process until having the desired solution with a time-efficient process. What it was a disadvantage for adiabatic annealing, converted into a new possibility for the diabatic annealing.

In [29], there is a more extensive analysis on the possibilities offered by diabatic quantum annealing. But some studies[32], seem to show that the optimal angle of QAOA approximates to the parametrization of a continuous annealing path, i.e. that it converges to a diabatic quantum annealing protocol. So, there is a good reason to be hopeful for the future of diabatic quantum annealing.

4 Simulation of a qubit

4.1 Introduction

The goal of the practical part of this project is to get an understanding to the most basic element of quantum computation, a qubit. We work with a stochastic environment, with quantum back action and continuous measurements involved. We will simulate a continuous measurement on a qubit with a Rabi drive. The Rabi drive is a type of cyclic behaviour given in certain two-level systems that induces the state to be oscillating. It usually occurs when a particle is in the presence of a field in its excitation frequency. In our system, the rotation will be undergoing in the y-axis. Therefore, as we will see, all states that start in the x-z plane will remain there.

4.2 Calculations

In this simulation we will consider only one measurement channel. So, as we saw before in Eq.15, for the particular case of $n = 1$, the equation is given by:

$$\mathrm{d}\rho = -i[H,\rho]\mathrm{d}t + \mathcal{D}[c]\rho\mathrm{d}t + \eta^{1/2}\mathcal{H}[c]\rho\mathrm{d}W \tag{30}$$

where the Hamiltonian (H) is defined by the Rabi drive in the y-axis $H = \frac{\omega}{2}Y$, the dissipative term ($\mathcal{D}[c]\rho$ or $\mathcal{L}\rho$) is given by the Lindbladian for a measurement in the z-axis [33], $\mathcal{D}[c]\rho = \mathcal{L}\rho = \frac{\Gamma_m}{2}(Z\rho Z - \rho)$ and the stochastic term is given by $\mathcal{H}[c]\rho = \sqrt{2\Gamma_m}\left(\frac{Z\rho+\rho Z}{2} - z\rho\right)$. Remember that we have set $\hbar = 1$. Notice that the amplitude of the Wiener process will depend on its variance. In our case, this variance is given by the *measurement time*: $\tau_m = \frac{1}{2\Gamma_m\eta}$.

To derive the equations we started with a simpler case, with only Rabi drive. The motion is described by the Von Neumann Eq.8, since there's only coherent evolution.
The state is written in terms of the Bloch vector as:

$$\rho(t) = \frac{1}{2}\left[\mathbf{I} + x(t)X + y(t)Y + z(t)Z\right] \tag{31}$$

The way to derive the equations is by differentiating on both sides over time, and applying the operator for which we want to know the equations of motion and make the trace over it, in order to get the time dependence of the expectation value of the operator.

$$\begin{cases} \dot{x} &= Tr(X\dot{\rho}) = Tr\left(X\frac{1}{i}[H,\rho]\right) = \omega z \\ \dot{y} &= Tr(Y\dot{\rho}) = Tr\left(Y\frac{1}{i}[H,\rho]\right) = 0 \\ \dot{z} &= Tr(Z\dot{\rho}) = Tr\left(Z\frac{1}{i}[H,\rho]\right) = -\omega x \end{cases} \tag{32}$$

We can clearly see that they set the equations of motion of a uniform cirular movement in the x-z plane, as expected from Rabi oscillations.

Then, we introduce the dissipation terms. We proceed as before, applying the Pauli matrices and

tracing over them.

$$\begin{aligned}
\dot{x}: &\quad Tr(X\mathcal{L}[Z]\rho) = Tr\left(X\left(\tfrac{\Gamma_m}{2}\left(Z\rho Z-\rho\right)\right)\right) = -\Gamma_m Tr(X\rho) = -\Gamma_m x \\
\dot{y}: &\quad Tr(Y\mathcal{L}[Z]\rho) = Tr\left(Y\left(\tfrac{\Gamma_m}{2}\left(Z\rho Z-\rho\right)\right)\right) = -\Gamma_m Tr(Y\rho) = -\Gamma_m y \\
\dot{z}: &\quad Tr(Z\mathcal{L}[Z]\rho) = Tr\left(Z\left(\tfrac{\Gamma_m}{2}\left(Z\rho Z-\rho\right)\right)\right) = 0
\end{aligned} \tag{33}$$

To perform the calculations we have used linearity($Tr(\alpha A + \beta B) = \alpha Tr(A) + \beta Tr(B)$) and cyclic property of the trace($Tr(ABC) = Tr(BCA) = Tr(CAB)$). Notice that x and y have a negative term in the derivative. This means that it will have an exponential decay along those axis from these terms. This phenomenon it's called *decoherence* and it's an important phenomenon in open quantum systems. Decoherence is formed due to quantum backaction of the measurement device. It brings the qubit to a mixed state (remember that the center of the Bloch sphere is the fully mixed state). Also, notice that since we are measuring along the z-axis, the decoherence doesn't affect the motion along this axis. Finally, we do the same with the stochastic terms.

$$\begin{aligned}
\dot{x}: &\quad Tr(X\mathcal{H}[c]\rho) = Tr\left(X\left(\tfrac{Z\rho+\rho Z}{2}-z\rho\right)\right) = -Tr(X\rho)Tr(Z\rho) = -xz \\
\dot{y}: &\quad Tr(Y\mathcal{H}[c]\rho) = Tr\left(Y\left(\tfrac{Z\rho+\rho Z}{2}-z\rho\right)\right) = -Tr(Z\rho)Tr(Y\rho) = -zy \\
\dot{z}: &\quad Tr(Z\mathcal{H}[c]\rho) = Tr\left(Z\left(\tfrac{Z\rho+\rho Z}{2}-z\rho\right)\right) = Tr(X\rho) + Tr(X\rho) - Tr(X\rho)Tr(X\rho) = 1-z^2
\end{aligned} \tag{34}$$

So, overall the equation of motion describing the state evolution of the system under continuous measurement is:

$$\begin{cases}
\dot{x} &= \omega z - \Gamma_m x - \sqrt{2\Gamma_m \eta}\; xz\frac{dW}{dt} \\
\dot{y} &= -\Gamma_m y - \sqrt{2\Gamma_m \eta}\; yz\frac{dW}{dt} \\
\dot{z} &= -\omega x + \sqrt{2\Gamma_m \eta}\left(1-z^2\right)\frac{dW}{dt}
\end{cases} \tag{35}$$

As we predicted, the states that start in the x-z plane stay enclosed in that surface their whole trajectory, since stochastic term for the y direction depends on the y component being non-zero at some initial time. So, this means $(x_0, 0, z_0) \to (x(t), 0, z(t))$. In the x component, we have an interesting behaviour. The first two terms have opposing behaviours, in the sense that the Rabi drive will be performing a motion that in certain conditions it will increase the value of x, while the dissipative term will always try to decrease it exponentially to 0. The stochastic part in the x

direction is analogous to the stochastic part in the direction of y. In the z component, the behaviour is completely different. The first term is the expected from a Rabi cycle, that will lead to a circular motion. However, notice that there's no decoherence. This is expected, because the measurement is along the z-axis and therefore the system tries to "pull" towards the eigenstates of the observable (since it's a Z gate, towards $|0\rangle$ *or* $|1\rangle$).

In general, we will see that the system has different regimes and that parameter affects its behaviour greatly and in different ways. The relation ω-Γ_m will be decisive for the x coordinate and, therefore, for the system.

4.3 The Pierre Rouchon Method

To perform our calculations, we have used a numerical method developed by Pierre Rouchon *et al.* in [34]. We have chosen this method because it gives a result contained in the space of semi-definite positive Hermitian matrices and has unitary trace ($Tr(\rho) = 1$). It is derived for a general scenario, that is the following. We have a measurement defined by the stochastic equation:

$$dy_t = \sqrt{\eta}\,\mathrm{Tr}\left(\left(\boldsymbol{L} + \boldsymbol{L}^\dagger\right)\boldsymbol{\rho}_t\right)dt + d\boldsymbol{W}_t \tag{36}$$

where $\boldsymbol{L}$ is the Lindblad operator, η is the efficiency of the measurement, dt is the timestep and dW_t is a Wiener process, formed by a Gaussian noise with variance equal to dt ($W_{dt} - W_0 \sim N(0, dt)$).

The system is governed by the Lindblad equation, written as:

$$\begin{aligned} d\boldsymbol{\rho}_t = &\left(-\tfrac{i}{\hbar}\left[\boldsymbol{H}, \boldsymbol{\rho}_t\right] + \textstyle\sum_\nu \boldsymbol{L}_\nu \boldsymbol{\rho}_t \boldsymbol{L}_\nu^\dagger - \tfrac{1}{2}\left(\boldsymbol{L}_\nu^\dagger \boldsymbol{L}_\nu \boldsymbol{\rho}_t + \boldsymbol{\rho}_t \boldsymbol{L}_\nu^\dagger \boldsymbol{L}_\nu\right)\right)dt \\ &+ \textstyle\sum_\nu \sqrt{\eta_\nu}\left(\boldsymbol{L}_\nu \boldsymbol{\rho}_t + \boldsymbol{\rho}_t \boldsymbol{L}_\nu^\dagger - \mathrm{Tr}\left(\left(\boldsymbol{L}_\nu + \boldsymbol{L}_\nu^\dagger\right)\boldsymbol{\rho}_t\right)\boldsymbol{\rho}_t\right)dW_{\nu,t} \end{aligned} \tag{37}$$

It is shown in his research[35] to be equivalent to:

$$\rho_{t+dt} = \frac{M_{dy_t}\rho_t M_{dy_t}^\dagger + \sum_\nu (1-\eta_\nu)\,\boldsymbol{L}_\nu \rho_t \boldsymbol{L}_\nu^\dagger dt}{\mathrm{Tr}\left(\boldsymbol{M}_{dy_t}\boldsymbol{\rho}_t \boldsymbol{M}_{dy_t}^\dagger + \sum_\nu (1-\eta_\nu)\,\boldsymbol{L}_\nu \boldsymbol{\rho}_t \boldsymbol{L}_\nu^\dagger dt\right)} \tag{38}$$

with

$$\boldsymbol{M}_{dy_t} = \boldsymbol{I} + \left(-\frac{I}{\hbar}\boldsymbol{H} - \frac{1}{2}\boldsymbol{L}_\nu^\dagger \boldsymbol{L}_\nu\right) dt + \sum_\nu \sqrt{\eta_\nu} dy_{\nu,t} \boldsymbol{L}_\nu \tag{39}$$

This method ensures that the solution remains in the semi-definite positive Hermitian matrices space, that it has a unique solution, that the trace is unitary ($Tr(\rho_{t+dt}) = 1$) and it provides a time-discretized approach for a solution. So, overall, it's a method that will ensure the solution is well-defined according to quantum mechanics. Order 4 Runge-Kutta methods could be also used to find approximate results at a similar computational cost, but they are not trace-preserving. That's why we have opted for this method in our project.

Notice that Eq.38 & Eq.39 are formulated for several observers (ν), and hence several Lindblad operators, but in our case we only use one inefficient measurement. By comparing Eq.37 with Eq.30 we can see that for our specific case, the Lindblad operator is:

$$L = \frac{\sqrt{\Gamma_m}}{2} Z \tag{40}$$

In this project, we mainly use the Hamiltonian of the Rabi cycles in the x-z plane($H = \frac{\omega}{2}Y$). But, we will make a comparison with a Rabi driven system along the x-y plane ($H = \frac{\omega}{2}Z$), so now the measurements and the Rabi drive are along the same axis.

4.4 Results

The calculations were done in reduced units. We set as a reference parameter the measurement strength: $\Gamma_m = 1$. The timestep was fixed at $dt = 5 \cdot 10^{-3}\Gamma_m$ and we varied the length of the simulation (N_t) depending on the situation, longer times for setups that had longer timescales and shorter times for setups with shorter ones.

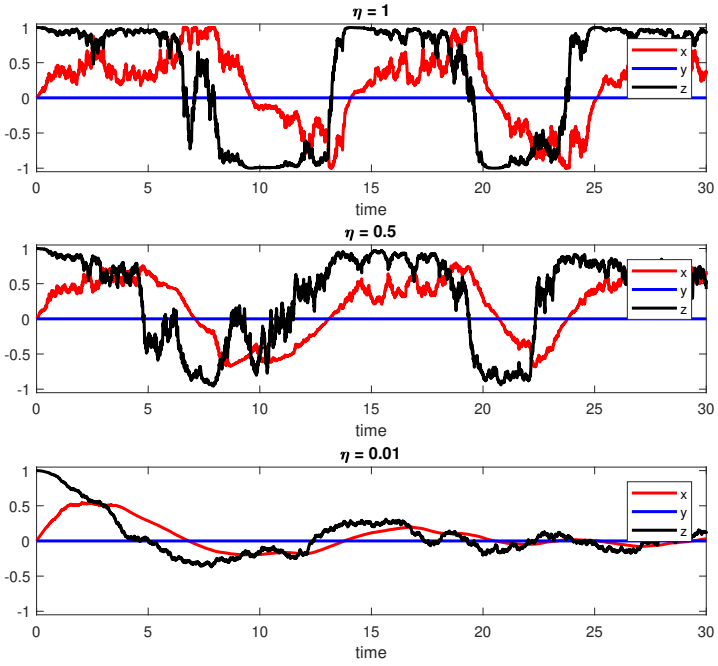

Figure 5: Trajectory of the state for $\omega = 0.5\Gamma_m$, $N_t = 6000$ and varying η: top $\eta = 1$, middle $\eta = 0.5$ and bottom $\eta = 0.01$

In these setups, we have a regime where ω and Γ_m are of the same order, so we get rich dynamics (that we will explain later). We have varied the efficiency of the measurement. The run at the top is one performed with an ideal measuring device, the one in the middle is done with an efficiency of 50% and the lower one is performed with a really inefficient device, with only 1% efficiency. As we can see from Eq.35, the efficiency parameter helps to modulate the amplitude of the stochastic term of the trajectory. On one hand, if the measuring device is perfect, the system exhibits its rich dynamics between the noise and the Rabi cycles. On the other hand, if the measuring device is really inefficient, the state tends to end in the center of the Bloch sphere, i.e. in a completely mixed state. The dissipative terms govern mainly the system. This means that an inefficient device will get a state more mixed. It's a problem for many applications, because for quantum computation we usually want the qubits to be more pure to be able to control them. This is the reason it is really important to achieve technological improvements in measuring detectors for qubit applications.

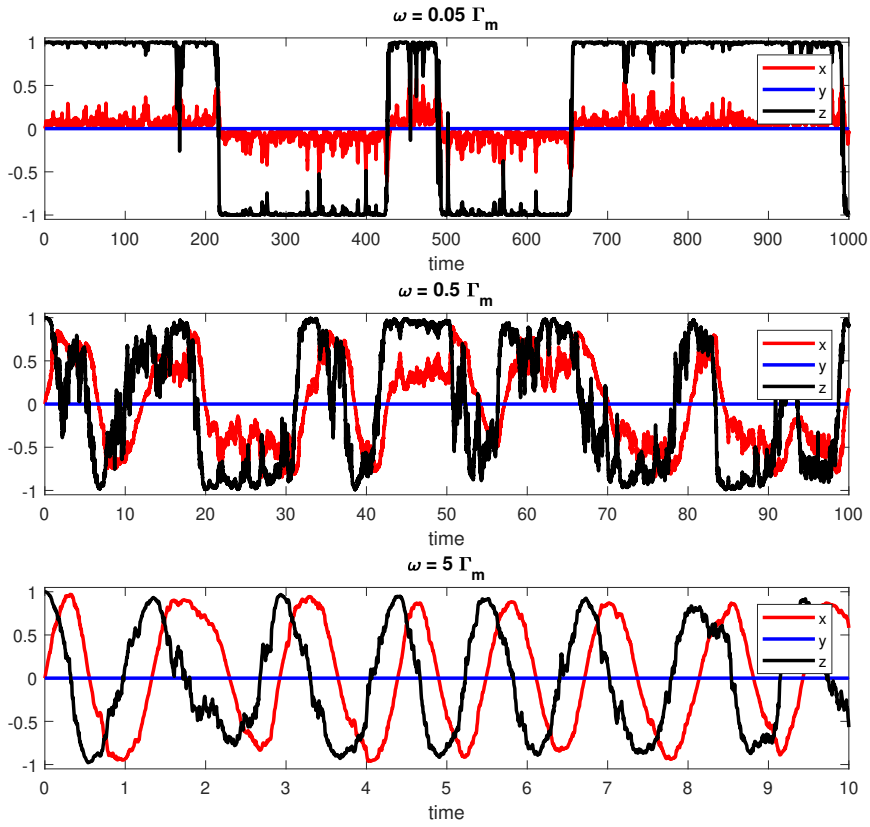

Figure 6: Trajectory of the state for $\eta = 0.6$ varying ω and N_t: top $\omega = 0.05\Gamma_m$, $N_t = 2 \cdot 10^5$, middle $\omega = 0.5\Gamma_m$, $N_t = 2 \cdot 10^4$ and bottom $\omega = 5\Gamma_m$, $N_t = 2 \cdot 10^3$

In Fig.7, we present three different setups. In this occasion we have let the measurement efficiency be a constant at a value of 60% and instead, we have varied the $\frac{\omega}{\Gamma_m}$ relation. For the lowest graphic, we had set a fast Rabi drive: $\omega = 5\Gamma_m$. The decoherence terms lose strength when compared against the Rabi drive. We see a cyclic motion in the x-z plane, with some disturbances. But one can clearly see the sinusoid pattern on the graph. In fact, in the limit case $\frac{\omega}{\Gamma_m} \to \infty$, we recover the equations

of the Rabi drive for the x and z components:

$$\begin{cases} \dot{x} &= \omega z \\ \dot{y} &= -\Gamma_m y - \sqrt{2\Gamma_m \eta}\; yz \frac{dW}{dt} \\ \dot{z} &= -\omega x \end{cases} \tag{41}$$

In the middle graph, we cannot longer see clearly the dynamics of the Rabi cycle. The stochastic terms have become prominent and there are large fluctuations. We can also notice that the z component starts to be of greater amplitude than the x component. This is something one couldn't appreciate in the lower graph scenario. So, the slower the Rabi cycles are compared to the measurement strength, the more the state tends to get closer to its eigenstates. In the top graph we have a measurement strength two orders of magnitude above the angular speed of the Rabi cycles: $\omega = 0.05\Gamma_m$. Here, we can appreciate that the qubit tends to "stick" to its eigenstates. This is the phenomenon called quantum Zeno effect that we explained in a previous section. The amplitude of x is fairly smaller than that of the z component and it seems that the system evolves by jumps from one eigenstate to the other one. In fact, in the limit $\frac{\omega}{\Gamma_m} \to 0$ we get the equations of a telegraph signal for the z component. The probability of jump after a jump is done is given by a Poisson point process Eq.42. The calculations are done in the Appendix A.

$$P(t) = \Gamma_J e^{-\Gamma_J t} \tag{42}$$

where $\Gamma_J = \frac{\omega^2}{\Gamma_m}$ is the jump rate and defines jump mean time as $\tau_J = \frac{1}{\Gamma_J} = \frac{\Gamma_m}{\omega^2}$.

4.5 Side remark

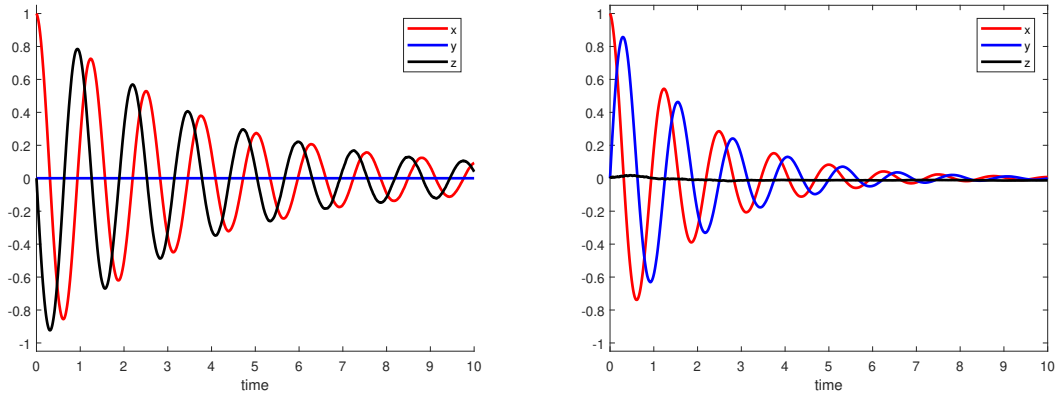

(a) $H = \frac{\omega}{2}Y$ (b) $H = \frac{\omega}{2}Z$

Figure 7: Averaged state of the system with respect to time for two different Hamiltonians

By looking at Fig.7, one could think that we are talking about similar systems, that act similarly, but that is not the case. They are the averaged results from several runs of two different setups. In fact, the behaviours of each system on a single run are shown in Fig.8. In both figures, the left graph is from a system where we measure and perform Rabi cycles in different axis, while in the right graphs we measure in the same axis as the Rabi cycle occurs. This is why we have used figures from single runs and not from averages. This behaviour occurs because the autocorrelation decays exponentially in time (see Appendix A), therefore, since all the stochastic variables are uncorrelated and independent, it will also decay exponentially as we average with realizations.

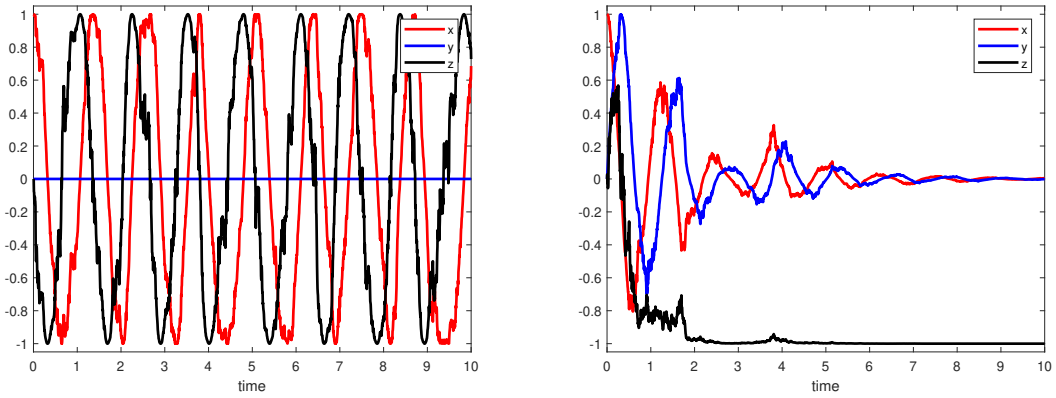

(a) $H = \frac{\omega}{2} Y$ (b) $H = \frac{\omega}{2} Z$

Figure 8: Single realizations for two different Hamiltonians

As a side note, in the case of Rabi drive axis being in the same direction as the measurement axis, there's a theorem that ensures that the system will end in an eigenstate and not jump [33].

Theorem. Consider the SME:

$$d\rho_t = -\frac{i}{\hbar}\left[\boldsymbol{H}, \boldsymbol{\rho}_t\right] dt + \frac{\Gamma_m}{4}\left(\sigma_z \boldsymbol{\rho}_t \sigma_{\mathbf{z}} - \boldsymbol{\rho}_t\right) dt + \frac{\sqrt{\eta\Gamma_m}}{2}\left(\sigma_{\mathbf{z}} \boldsymbol{\rho}_t + \boldsymbol{\rho}_t \sigma_{\mathbf{z}} - 2\,\mathrm{Tr}\left(\sigma_{\mathbf{z}} \boldsymbol{\rho}_t\right) \boldsymbol{\rho}_t\right) dW_t \tag{43}$$

with $\boldsymbol{H} = \frac{\omega_{\mathrm{eg}}}{2} Z$ and $\eta > 0$.

For any initial state ρ_0, the solution ρ_t converges almost surely as $t \to \infty$ to one of the states $|g\rangle\langle g|$ or $|e\rangle\langle e|$.

The probability of convergence to $|g\rangle\langle g|$ (respectively $|e\rangle\langle e|$) is given by $p_g = \mathrm{Tr}\left(|g\rangle\langle g|\rho_0\right)$ (respectively $\mathrm{Tr}\left(|e\rangle\langle e|\rho_0\right)$)

The convergence rate is given by $\eta\Gamma_M/2$.

5 Conclusion

In this project, we have done a broad survey to quantum annealing and its possibilities for the near future applications. Diabatic quantum annealing seems to be one of the most promising subjects

of research on the field of quantum simulations to achieve quantum supremacy, since adiabatic quantum annealing is too restrictive and the non-stoquasticity doesn't guarantee better results. We have also described some of the most important concepts on this topic, as an introduction to this subject. From this point, we have set an introductory base to be able to follow the general lines of current research. We have also made a simulation of the basic unit of quantum computation, a qubit, in a general setup that takes into account imperfections on the measurement and random noise generation while the qubit is also being driven with a coherent field. This demonstrated the competition between coherent evolution and measurement that is summarized in the Quantum Zeno effect. We have compared the different interactions within our system. However, this project was merely an introduction to this topic, since one can go more in-depth into several fields, such as multiqubit systems, qubit control, state purification, error correction... So, overall, we consider we have accomplished our objective for this project and await to see how will quantum annealing develop in the next few years.

6 Acknowledgements

First, I would like to thank Prof. K. Birgitta Whaley for guiding me during all this project. The scheduled meetings were a crucial part to understanding many topics in this field that was completely new for me and the conferences and meetings with other researchers was a huge inspiration to the potential that quantum computing can bring us.

I would also want to express my gratitude to Prof. Jordi Boronat for keeping track of my efforts and for putting me in contact with the research group.

A special thanks to Dr. Song Zhang for helping me on the simulation and to Dr. Juan Atalaya for aiding me on the calculations and theoretical aspects of the project. Also, thanks to the members of the Whaley Research group for their kindness and support shown to me in the University of California Berkeley. You made me all feel like part of the group, even if it was for a few months.

Lastly, due to the situation with the coronavirus and the confinement, I have to thank dearly my family for giving me support all these months and taking care of me in these trying times.

A Autocorrelation and the Telegraph signal

We start deriving the signal as a Poisson Point process, in the limit $\frac{\omega}{\Gamma_m} \to 0$. We have seen that the signal jumps between two values, so it either has two values: $|0\rangle$ or $|1\rangle$. Since it's symmetric for both halves of the Bloch sphere, we can assume we start on one of those states just after a jump ($t = 0$) and calculate the probability to jump in the time t ($P(t)$). It is convenient to discretize time and then perform the limit. In a certain dt one has a probability to jump of $\Gamma_J dt$ and, therefore, a probability to stay of $1 - \Gamma_J dt$. Then, after N steps, the probability to jump will be the probability of not jumping $N - 1$ times and jumping one time:

$$P(N\Delta t) = (1 - \Gamma_J \Delta t)^{N-1} \Gamma_J \tag{44}$$

Now, if we keep the value $N\Delta t = t$ constant and take the limit $dt \to 0$:

$$P(t) = \lim_{dt\to 0} (1 - \Gamma_J dt)^{N-1} \Gamma_J = \lim_{dt\to 0} (1 - \Gamma_J dt)^{\frac{t}{dt}-1} \Gamma_J = e^{-\Gamma_J t} \Gamma_J \tag{45}$$

We obtain the probability distribution of a Poisson point process. Now we have to derive what is the value of the jump rate Γ_J. To do this we have to look at our signal and calculate the relaxation function. The relaxation function can be found by finding the autocorrelation of our signal [36]. So, we start by calculating $K(t) = \langle z(t)z(0)\rangle$. To do so, we derive it on both sides to work with $\dot{z}$ that we have an expresison we can use (Eq.35).

$$\dot{K}(t) = \langle \dot{z}(t) z_0 \rangle = \left\langle \left(-\omega x(t) + \sqrt{2\Gamma_m \eta} \left(1 - z^2\right) \frac{dW}{dt} \right) z(0) \right\rangle = -\omega \langle x(t) z_0 \rangle + \sqrt{2\Gamma_m \eta} \left\langle \left(1 - z^2\right) \frac{dW}{dt} z_0 \right\rangle \tag{46}$$

Since the noise $\frac{dW}{dt}$ is uncorrelated, the second term will have mean 0 $\left\langle \left(1 - z^2\right) \frac{dW}{dt} z_0 \right\rangle = 0$. So,

$$\dot{K}(t) = -\omega \langle x(t) z_0 \rangle \tag{47}$$

Now, we perform another derivation. Again, we can work with $\dot{x}$ from Eq.35 but not x directly.

That's why we use this method of derivating.

$$\ddot{K}(t) = -\omega\langle\dot{x}(t)z_0\rangle = -\omega\left\langle\left(\omega z - \Gamma_m x - \sqrt{2\Gamma_m\eta}\; xz\frac{dW}{dt}\right)z_0\right\rangle \tag{48}$$

Again, we can see that the last term has Gaussian uncorrelated noise, so we will have:

$$\ddot{K}(t) = -\omega\left\langle\left(\omega z - \Gamma_m x\right)z_0\right\rangle = -\omega^2\langle z(t)z_0\rangle + \omega\Gamma_m\langle x(t)z_0\rangle = -\omega^2 K(t) + \omega\Gamma\frac{\dot{K}(t)}{-\omega} \tag{49}$$

This give us an ordinary differential equation with constant coefficients.

$$\ddot{K}(t) + \Gamma_m\dot{K}(t) + \omega^2 K(t) = 0 \tag{50}$$

So, after imposing the initial conditions $K(0) = z_0^2$ and $\dot{K}(0) = 0$,the autocorrelation function will be

$$K(t) = C_+\exp\left(\lambda_+ t\right) + C_-\exp\left(\lambda_- t\right) \tag{51}$$

With $\lambda_\pm = \frac{-\Gamma_m \pm\sqrt{\Gamma_m^2-(2\omega)^2}}{2}$ and $C_\pm = \frac{-\Gamma_m \mp\sqrt{\Gamma_m^2-(2\omega)^2}}{\sqrt{\Gamma_m^2-(2\omega)^2}}z_0^2$ As stated in Kubo theory [37], for a generalized relaxation function:

$$\phi_1(t) = G_+(t) - G_-(t) \tag{52}$$

with G_ϵ being:

$$G_\varepsilon(t) = \frac{1+\varepsilon Y + i\eta X}{2Y}\exp\left[-(1-\varepsilon Y)\frac{|t|}{2\tau_c}\right] \tag{53}$$

where $Y^2 = 1 - X^2 + 2i\eta X$ and $X = \Omega\tau_c$. Since it's a symmetrical process $\eta = 0$. In our case, if we want to compare $\varphi(t)$ and $K(t)$ we have the following relations (after a few trivial algebraic operations, which we have not included): $\tau_c = \frac{1}{\Gamma_m}$, $Y = \sqrt{1-\left(\frac{2\omega}{\Gamma_m}\right)^2}$, $X = \frac{2\omega}{\Gamma_m}$, $\Omega = 2\omega$ and a constant $k = 2z_0^2$. In the motional narrowing regime ($\Gamma_m >> \omega$), one can approximate it, via Taylor expansion as in [37] to the equation:

$$\phi_1(t) \sim \exp\left(-\frac{\Omega^2\tau_c|t|}{4}\right) \tag{54}$$

Substituting by our values using the relations found before it reads:

$$\phi_1(t) \sim \exp\left(-\frac{(2\omega)^2|t|}{4\Gamma_m}\right) = \exp\left(-\frac{\omega^2}{\Gamma_m}|t|\right) \tag{55}$$

So, looking back at Eq.45 for a Poisson process and compare the terms, one can verify that

$$\Gamma_J = \frac{\omega^2}{\Gamma_m} \tag{56}$$

B References

[1] Heshami, Khabat; England, Duncan G.; Humphreys, Peter C.; Bustard, Philip J.; Acosta, Victor M.; Nunn, Joshua; Sussman, Benjamin J. (2016-11-12). *"Quantum memories: emerging applications and recent advances"*. Journal of Modern Optics. 63 (20): 2005–2028. doi:10.1080/09500340.2016.1148212. ISSN 0950-0340. PMC 5020357. PMID 27695198

[2] Joschka Roffe (2019-07-25). *Quantum Error Correction: An Introductory Guide*. Contemporary Physics Journal 2019. arXiv:1907.11157 doi:10.1080/00107514.2019.1667078

[3] Markoff, John (September 27, 2015). *"Smaller, Faster, Cheaper, Over: The Future of Computer Chips"*. The New York Times. Retrieved September 28, 2015

[4] Dubash, Manek (2005-04-13). *"Moore's Law is dead, says Gordon Moore"*. Techworld. Retrieved 2006-06-24

[5] Arute, F., Arya, K., Babbush, R. et al. *"Quantum supremacy using a programmable superconducting processor"*. Nature 574, 505–510 (2019). https://doi.org/10.1038/s41586-019-1666-5

[6] https://www.ibm.com/quantum-computing/

[7] K.Jacobs and D. Steck *"A straightforward introduction to continuous quantum measurement"*. Contemporary Physics, Vol. 47, No. 5, September–October 2006, 279 – 303

[8] S. Hacohen-Gourgy, L. P. García-Pintos, L. S. Martin, J. Dressel, and I. Siddiqi *"Incoherent qubit control using the quantum Zeno effect"*. arXiv:1706.08577v1 (2017)

[9] E.G. Rieffel and W. H. Polak. *Quantum Computing: A Gentle Introduction*. MIT Press, 2011.

[10] Boyd, Stephen P.; Vandenberghe, Lieven (2004).Convex Optimization(pdf). Cambridge UniversityPress. p. 129. ISBN 978-0-521-83378-3

[11] Schrijver, Alexander (2003).Combinatorial Optimization: Polyhedra and Efficiency. Algorithms andCombinatorics. 24. Springer. ISBN 9783540443896

[12] Bellman (1960), Bellman (1962), Held Karp (1962)

[13] Rego, C esar; Gamboa, Dorabela; Glover, Fred; Osterman, Colin (2011),"Traveling salesman prob-lem heuristics: leading methods, implementations and latest advances", European Journal of Oper-ational Research, 211 (3): 427–441, doi:10.1016/j.ejor.2010.09.010, MR 2774420

[14] M. Born and V. A. Fock (1928)."Beweis des Adiabatensatzes". Zeitschrift f ur Physik A. 51 (3–4):165–180. Bibcode:1928ZPhy...51..165B. doi:10.1007/BF01343193

[15] E. Crosson, E. Farhi, C.Y-Y. Lin, H-H. Lin, and P. Shor,"Different Strategies for Optimizationusing the Quantum Adiabatic Algorithm", arXiv:1401.7320

[16] E. Farhi, J. Goldstone, and S. Gutmann,"A Quantum Approximate Optimization Algorithm"(2014),arXiv:1411.4028

[17] Barak, Boaz; Moitra, Ankur; O'Donnell, Ryan; Raghavendra, Prasad; Regev, Oded; Steurer, David;Trevisan, Luca; Vijayaraghavan, Aravindan; Witmer, David; Wright, John (2015)."Beating the random assignment on constraint satisfaction problems of bounded degree". arXiv:1505.03424 [cs.CC]

[18] Alberto Peruzzo, Jarrod McClean, Peter Shadbolt, Man-Hong Yung, Xiao-Qi Zhou, Peter J. Love,Alan Aspuru-Guzik, and Jeremy L. O'Brien. "A variational eigenvalue solver on a photonic quantumprocessor". Nature Communications, 5(1), July 2014

[19] Hadfield, Stuart and Wang, Zhihui and O'Gorman, Bryan and Rieffel, Eleanor and Venturelli, Davide and Biswas, Rupak. "From the Quantum Approximate Optimization Algorithm to a Quantum Alternating OperatorAnsatz"(2019), DOI:10.3390/a12020034

[20] Guillaume Verdonand Michael Broughton and Jarrod R. McClean and Kevin J. Sung and Ryan Babbush and ZhangJiang and Hartmut Neven and Masoud Mohseni "Learning to learn with quantum neural networks via classical neural networks" (2019) arXiv: 1907.05415

[21] Jarrod R McClean, Sergio Boixo, Vadim N Smelyanskiy, Ryan Babbush, and Hartmut Neven "Barren plateaus in quantum neural network training landscapes" .Nature communications, 9(1):4812, 2018

[22] Sergey Bravyi, "Monte carlo simulation of stoquastic hamiltonians", Quantum Information and Computation, Vol. 15, No. 1314 (2015) 1122–1140

[23] Sergei V. Isakov, Guglielmo Mazzola, Vadim N. Smelyan-skiy, Zhang Jiang, Sergio Boixo, Hartmut Neven, and Matthias Troyer, "Understanding quantum tunneling through quantum monte carlo simulations," Phys. Rev. Lett. 117, 180402 (2016)

[24] Elizabeth Crosson, Tameem Albash, Itay Hen and A. P. Young, "De-Signing Hamiltonians for Quantum Adiabatic Optimization" arXiv:2004.07681v1

[25] Yuki Susa, Johann F. Jadebeck, and Hidetoshi Nishimori, "Relation between quantum fluctuations and the performance enhancement of quantum annealing in a nonstoquastic hamiltonian," Phys. Rev. A 95, 042321 (2017)

[26] *"Quantum Approximate Optimization Algorithm: Performance, Mechanism, and Implementation on Near-Term Devices"*, Leo Zhou,1, Sheng-Tao Wang,1, † Soonwon Choi,1, 2 Hannes Pichler,3, 1 and Mikhail D. Lukin1 arXiv:1812.01041v1

[27] Tameem Albash and Daniel A. Lidar, *"Adiabatic Quantum Computation"*, Reviews of Modern Physics, 90, JANUARY–MARCH 2018

[28] B. Heim, T. F. Rønnow, S. V. Isakov and M. Troyer, *"Quantum versus classical annealing of Ising spin glasses"* Science 348, pp. 215–217 (2015)

[29] E.J. Crosson and D.A.Lidar, *"Prospects for Quantum Enhancement with Diabatic Quantum Annealing"*, arXiv:2008.09913v1 2020-22-08

[30] S. Jansen, M.-B. Ruskai, and R. Seiler, "Bounds for the adiabatic approximation with applications to quantum computation",J. Math. Phys.48, 102111 (2007) arXiv:quant-ph/0603175

[31] S. P. Jordan, D. Gosset, and P. J. Love, "Quantum-Merlin-Arthur–complete problems for stoquastic Hamiltonians and Markov matrices", Physical Review A 81, 032331 (2010).

[32] L. T. Brady, C. L. Baldwin, A. Bapat, Y. Kharkov, and A. V. Gorshkov, "Optimal protocols in quantum annealing and qaoa problems," (2020), arXiv:2003.08952

[33] H. M. Wiseman and G. J. Milburn, Quantum measurement and control (Cambridge university press, 2009).

[34] H. B. Silveira, P. S. Pereira da Silva and P. Rouchon, "A stochastic Lyapunov feedback technique for propagator generation of quantum systems on U(n)," 2013 European Control Conference (ECC), Zurich, 2013, pp. 2712-2716, doi: 10.23919/ECC.2013.6669234.

[35] Amini, Hadis Pellegrini, Clement Rouchon, Pierre. (2013). "Stability of continuous-time quantum filters with measurement imperfections". Russian Journal of Mathematical Physics. doi: 21. 10.1134/S1061920814030029. :arXiv:1312.0418

[36] A. Berthelot, C. Voisin, C. Delalande, Ph. Roussignol, R. Ferreira, G. Cassabois, "From Random Telegraph to Gaussian Stochastic Noises: Decoherence and Spectral Diffusion in a Semiconductor Quantum Dot", Advances in Mathematical Physics, vol. 2010, Article ID 494738, 13 pages, 2010. https://doi.org/10.1155/2010/494738

[37] R. Kubo, "A stochastic theory of line-shape and relaxation," in Fluctuation, Relaxation and Resonance in Magnetic Systems, D. Ter Haar, Ed., p. 23, Oliver and Boyd, Edinburgh, UK, 1962